27. F. Cappa, Y. Guglielmi, J. Virieux, *Geophys. Res. Lett.* **34**, L05301 (2007).
28. Y. Ben-Zion, J.-P. Ampuero, *Geophys. J. Int.* **178**, 1351 (2009).
29. M. Bohnhoff, M. D. Zoback, *J. Geophys. Res.* **115**, B11305 (2010).
30. F. Cappa, Y. Guglielmi, P. Fénart, V. Merrien-Soukatchoff, A. Thoraval, *Int. J. Rock Mech. Min. Sci.* **42**, 287 (2005).
31. J.-H. Hung *et al.*, *Tectonophysics* **466**, 307 (2009).

Acknowledgments: We thank C. Y. Wang for operational support for the TCDP site. This study benefited from discussions with H. Kanamori, M. Campillo, and T.-R. Alex Song. The TCDP BHS data are available to the public at the Data Center of the Taiwan Earthquake Research Center (TECDC) (http://tecws.earth.sinica.edu.tw/TCDP). This project is supported by National Science Council of Taiwan, NSC 100-2119-M-008 -031, and Ministry of Education 100G901-26 at National Central University.

Supplementary Materials
www.sciencemag.org/cgi/content/full/337/6093/459/DC1
Materials and Methods
Figs. S1 to S7
Table S1

19 March 2012; accepted 5 June 2012
10.1126/science.1222119

Adenylate Cyclases of *Trypanosoma brucei* Inhibit the Innate Immune Response of the Host

Didier Salmon,[1,2]*† Gilles Vanwalleghem,[1]† Yannick Morias,[3,4] Julie Denoeud,[5] Carsten Krumbholz,[6] Frédéric Lhommé,[7] Sabine Bachmaier,[6] Markus Kador,[6] Jasmin Gossmann,[6] Fernando Braga Stehling Dias,[1,2] Géraldine De Muylder,[1] Pierrick Uzureau,[1] Stefan Magez,[4,8] Muriel Moser,[5] Patrick De Baetselier,[3,4] Jan Van Den Abbeele,[9] Alain Beschin,[3,4] Michael Boshart,[6]* Etienne Pays[1,10]*

The parasite *Trypanosoma brucei* possesses a large family of transmembrane receptor–like adenylate cyclases. Activation of these enzymes requires the dimerization of the catalytic domain and typically occurs under stress. Using a dominant-negative strategy, we found that reducing adenylate cyclase activity by about 50% allowed trypanosome growth but reduced the parasite's ability to control the early innate immune defense of the host. Specifically, activation of trypanosome adenylate cyclase resulting from parasite phagocytosis by liver myeloid cells inhibited the synthesis of the trypanosome-controlling cytokine tumor necrosis factor–α through activation of protein kinase A in these cells. Thus, adenylate cyclase activity of lyzed trypanosomes favors early host colonization by live parasites. The role of adenylate cyclases at the host-parasite interface could explain the expansion and polymorphism of this gene family.

The protozoan flagellate *Trypanosoma brucei* infects a wide range of mammals, including humans, where it causes sleeping sickness. Bloodstream parasites are coated with a glycosylphosphatidylinositol (GPI)–anchored antigen termed variant surface glycoprotein (VSG) (*1*). Upon cellular stress, including cell lysis, activation of a GPI-specific phospholipase C (VSG lipase) triggers release of soluble VSG (*2*). Massive VSG release at the peak of parasitaemia contributes to interferon-γ (IFN-γ)–dependent tumor necrosis factor–α (TNF-α) synthesis by macrophages and high TNF-α serum levels, but early in infection, myeloid cells recruited

[1]Laboratory of Molecular Parasitology, Institute for Molecular Biology and Medicine (IBMM), Université Libre de Bruxelles, 12, rue des Professeurs Jeener et Brachet, B6041 Gosselies, Belgium. [2]Institute of Medical Biochemistry, Centro de Ciências e da Saude, Federal University of Rio de Janeiro, Avenida General Trompowsky, Rio de Janeiro 21941-590, Brazil. [3]Myeloid Cell Immunology Laboratory, Vlaams Instituut voor Biotechnologie, Brussels, Belgium. [4]Cellular and Molecular Immunology Unit, Vrije Universiteit Brussel, Brussels, Belgium. [5]Laboratory of Immunobiology, IBMM, Université Libre de Bruxelles, Gosselies, Belgium. [6]Biocenter, Section Genetics, Ludwig-Maximilians-Universität München, Martinsried, Germany. [7]Center for Microscopy and Molecular Imaging, Gosselies, Belgium. [8]Department of Structural Biology, VIB, Brussels, Belgium. [9]Department of Biomedical Sciences, Unit of Veterinary Protozoology, Institute of Tropical Medicine Antwerp, Antwerp, Belgium. [10]Walloon Excellence in Life Sciences and Biotechnology (WELBIO), Wavre, Belgium.

*To whom correspondence should be addressed. E-mail: salmon@bioqmed.ufrj.br (D.S.); boshart@lmu.de (M.B.); epays@ulb.ac.be (E.P.)
†These authors contributed equally to this work.

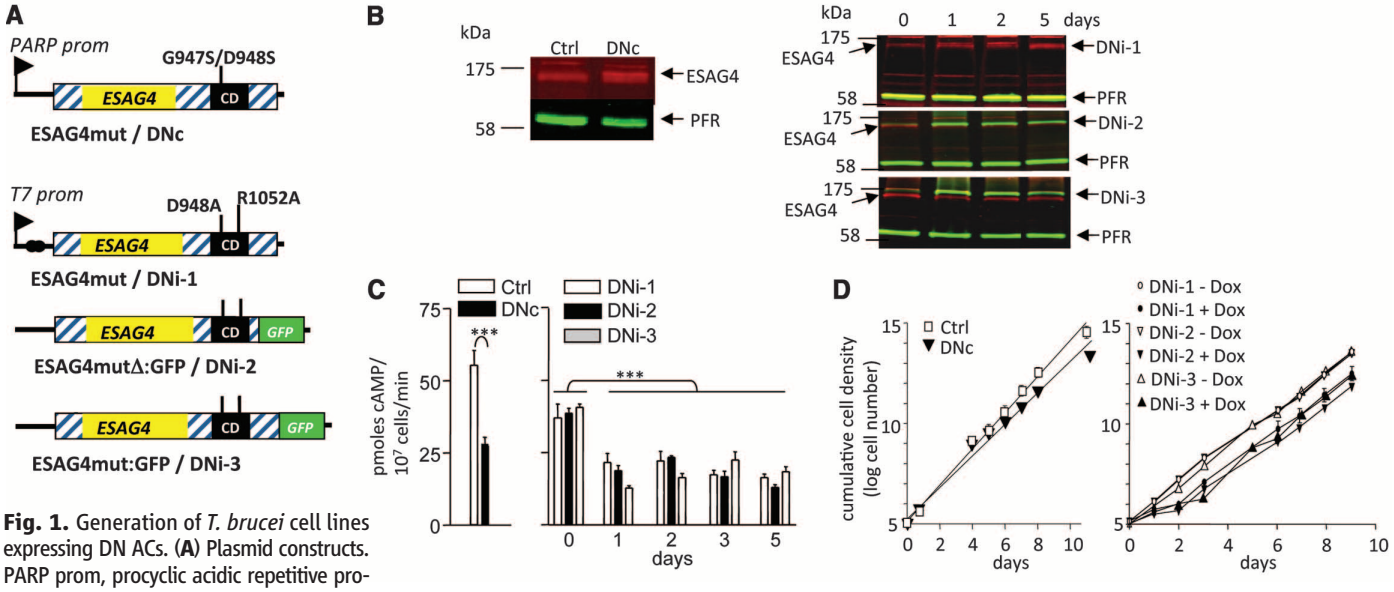

Fig. 1. Generation of *T. brucei* cell lines expressing DN ACs. (**A**) Plasmid constructs. PARP prom, procyclic acidic repetitive protein promoter; CD, catalytic domain. In DNi-2, the ESAG4 C terminus is truncated by 112 amino acids. (**B**) Immunoblot evidence for ESAG4 expression in pleomorphic DNc and monomorphic DNi parasites. Loading control: PFR, paraflagellar rod protein; d, day after doxycyclin (Dox) induction. (**C**) AC activity (cAMP synthesis), measured by swell dialysis after pH 5.5 treatment (*2*). AC activity of uninduced DNi parasites remained constant during the entire incubation period. (**D**) In vitro growth rate of the different cell lines. In this and the following figures, control (Ctrl) trypanosomes are transgenic pleomorphic trypanosomes containing an *ESAG4*-free plasmid (pTSARib0), and the values are means of at least three independent experiments (error bars, mean ± SEM). $*P < 0.05$, $**P < 0.01$, $***P < 0.001$ (Student-Newman-Keuls post hoc analysis of variance).

in liver and spleen already synthesize TNF-α independently from IFN-γ (*3*, *4*). Although involved in early trypanosome growth control, TNF-α also contributes to tissue pathogenicity during chronic infection (*5*–*7*).

Unlike related kinetoplastids developing intracellularly (*T. cruzi* and *Leishmania*), extracellular African trypanosomes (*T. brucei*, *T. congolense*, and *T. vivax*) show a remarkable expansion of receptor-like adenylate cyclases (ACs) without evidence for isoform orthologs between species (fig. S1). The *T. brucei* genome encodes more than 80 ACs, many of which were detected at the cell surface (*8*–*10*). The prototype gene of this family, termed *ESAG4* (expression site–associated gene 4), is included in polycistronic *VSG* transcription units, in contrast to the other genes termed *GRESAG4*s (genes related to *ESAG4*) (*10*, *11*). All ACs share a similar structure, with a large extracellular domain and a conserved intracellular catalytic domain, the dimerization of which is required for activity (*8*, *12*, *13*). Although the basal cellular cyclic adenosine monophosphate (cAMP) concentration is extremely low (~0.67 μM) (table S1), stress, such as acid treatment or osmotic lysis, activates ACs to produce ~250 times the basal cellular content per minute (*2*, *14*, *15*). AC and VSG lipase activities are triggered simultaneously but independently (*2*). Apart from ESAG4 involvement in cytokinesis (*10*), the function of *T. brucei* ACs is unknown.

To develop a dominant-negative (DN) approach, the catalytic domain of ESAG4 was inactivated by mutagenesis of key residues (*16*). A pleomorphic *T. brucei* clone was transformed for constitutive expression of the G947S/D948S mutant (DNc cell line), and three monomorphic

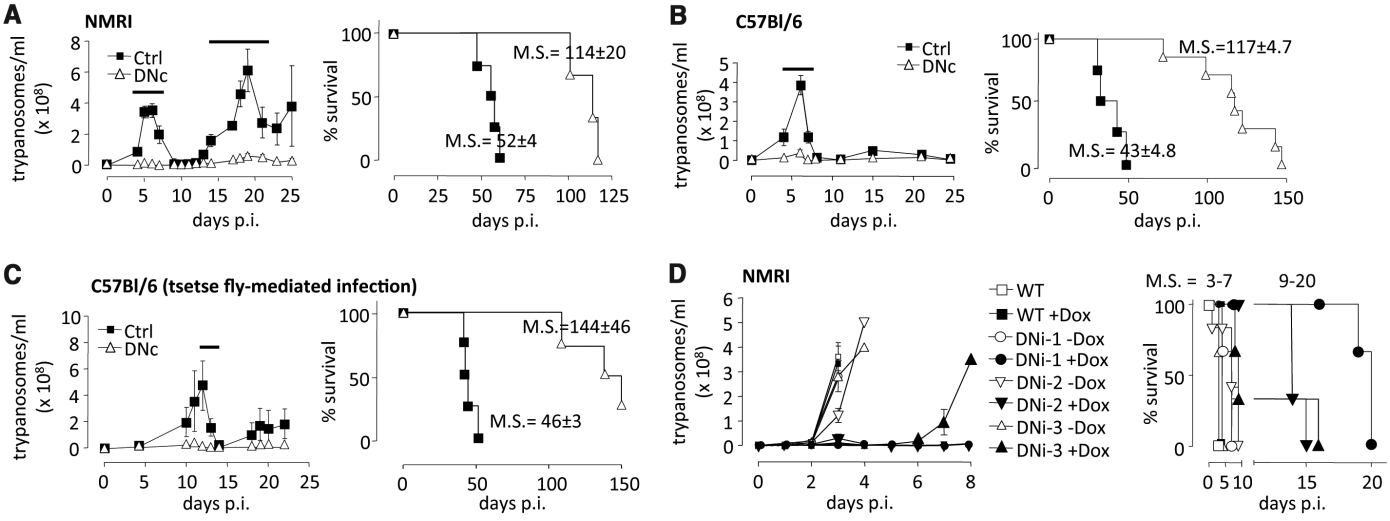

Fig. 2. Increased host capacity to control DN AC parasites. (**A** to **C**) Parasitaemia and survival time of different mice inoculated with pleomorphic control or DNc parasites by syringe [(A) and (B)] or infected tsetse flies (C). (**D**) Parasitaemia and survival time of NMRI mice inoculated by syringe with monomorphic WT or DNi parasites. M.S., median survival time. In this and the following figures, the bars above the parasitaemia graphs highlight significant differences between Ctrl and DNc or the respective comparison ($P < 0.05$).

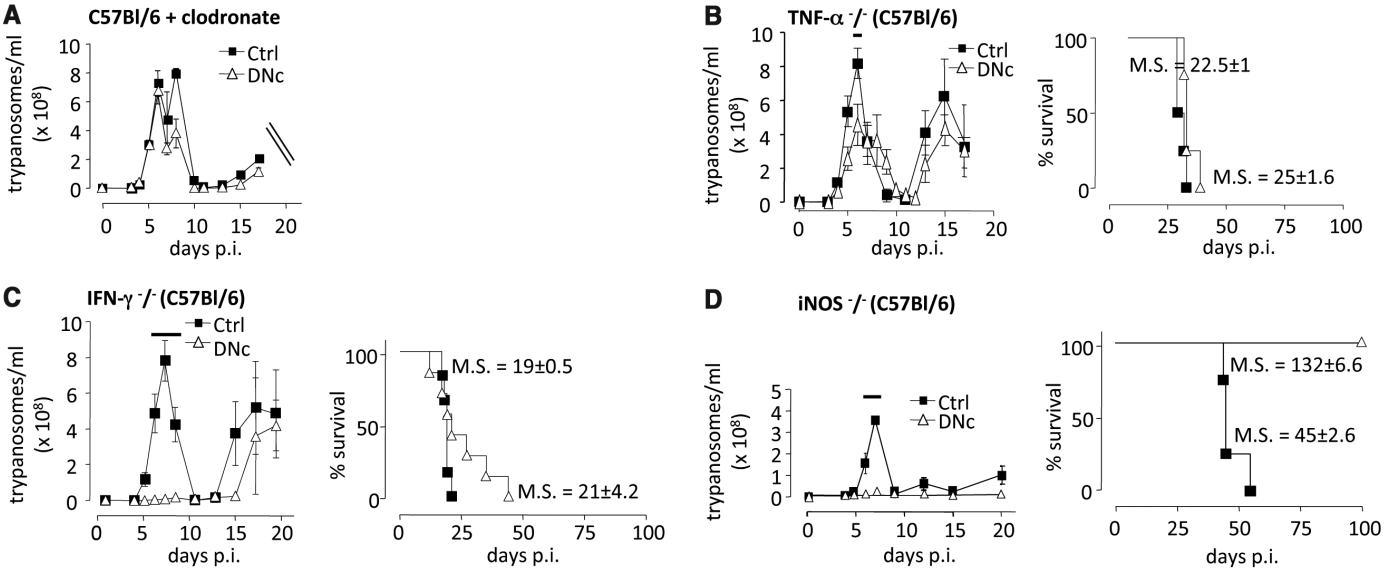

Fig. 3. Involvement of phagocytes and TNF-α in host capacity to control trypanosomes. (**A** to **D**) Parasitaemia and survival time of C57Bl/6 mice treated with clodronate-containing liposomes or deficient in TNF-α, IFN-γ, or iNOS, after inoculation with pleomorphic control or DNc parasites. The survival time of infected clodronate-treated mice was not determined.

trypanosome lines were generated for doxycycline-inducible expression of the D948A/R1052A mutant, with or without a C-terminal green fluorescent protein (GFP) tag (DNi-1, -2, and -3) (Fig. 1, A and B). The GFP-tagged DNi proteins showed the expected surface localization (*17*) (fig. S2). In DNc and induced DNi parasites, total AC activity, measured under stress conditions, was reduced by ~50% (Fig. 1C).

In culture, DNc growth was slightly reduced compared with control cells (Fig. 1D). Upon induction, the three DNi cell lines showed transient (~2 days) growth retardation and cytokinesis abnormalities (Fig. 1D and fig. S3A). Reversion correlated with up-regulation of *GRESAG4.1* expression, which was also seen in DNc (fig. S3B) and *ESAG4* knock-out parasites (*10*). In mice, DN AC expression strongly affected the infection pattern. After parasite inoculation by either intraperitoneal syringe-mediated injection or the bite of infected tsetse flies, DNc parasitaemia was considerably lower than control parasitaemia, and the host survival time was longer (Fig. 2, A to C). Serial DNc passaging in mice led to reversion of parasitaemia to control levels, linked to the loss of the DN *AC* transgene and recovery of AC activity (fig. S4). The DNc infection phenotype was mimicked by DNi parasites. Without induction, the three DNi lines killed mice after 3 to 4 days, as expected for monomorphic parasites (Fig. 2D). In contrast, doxycyclin induction led to drastic reduction of parasitaemia and prolongation of host survival time, whereas doxycyclin itself had no effect on wild-type (WT) parasite infection (*18*) (Fig. 2D).

The DNc infection pattern was largely conserved in mice deficient in either T lymphocytes (nude), T + B lymphocytes (severe combined immunodeficiency), or B lymphocytes (immunoglobulin μ-chain defective) (fig. S5). In contrast, DNc parasitaemia strongly increased in WT mice injected with clodronate-containing liposomes, indicating a crucial role for phagocytic

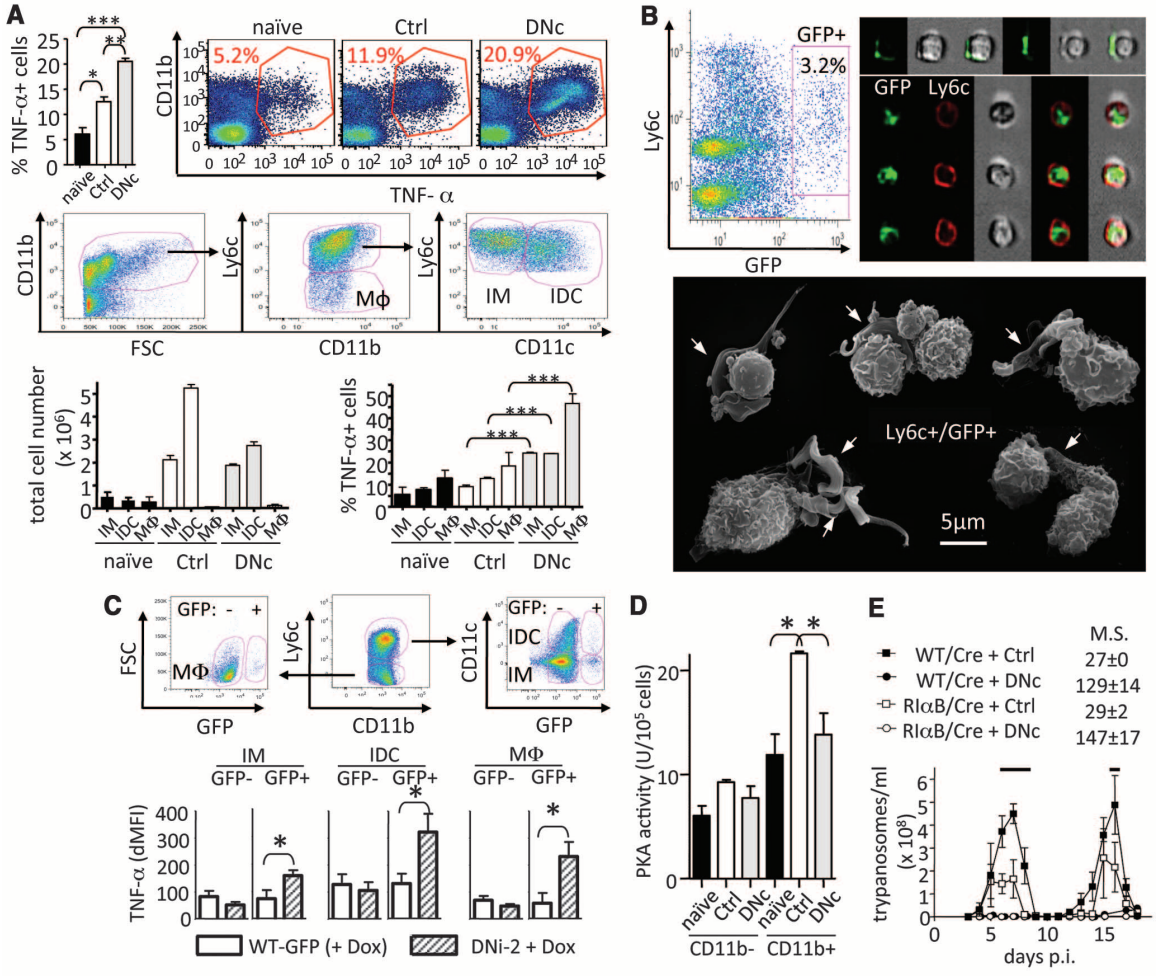

Fig. 4. Modulation of TNF-α synthesis after trypanosome infection. (**A**) Measurement of TNF-α^+ cells in total live nonparenchymal liver cells (top, mean values from three experiments and representative flow cytometry profiles) and in liver IMs ($CD11b^+/Ly6c^+/CD11c^-$), IDCs ($CD11b^+/Ly6c^+/CD11c^+$), and macrophages (MΦ) ($CD11b^+/Ly6c^-/CD11c^-$) (middle, gating strategy illustrated for DNc-infected mice; bottom, mean number of IM, IDC, and MΦ, and percentage of TNF-α^+ cells thereof, from three experiments) of C57Bl/6 mice at day 4 p.i. with pleomorphic control or DNc parasites. (**B**) Imaging of liver $Ly6C^+/GFP^+$ myeloid cells from C57Bl/6 mice at day 3 p.i. with GFP-labeled monomorphic WT trypanosomes. (Left) The gating of $Ly6C^+/GFP^+$ cells by Imagestream analysis. (Right and Bottom) Representative examples of $Ly6c^+/GFP^+$ cells with surface-bound or internalized parasites, seen by Imagestream and scanning electron microscopy, respectively (arrows point to myeloid cell–associated trypanosomes). (**C**) TNF-α levels in liver myeloid cells of C57Bl/6 mice at day 3 p.i. with GFP-expressing monomorphic WT trypanosomes or induced DNi-2 parasites, determined as mean fluorescence intensity difference (dMFI) between antibodies to TNF-α and isotype control antibodies. The gating strategy is illustrated for WT-infected mice. (**D**) PKA activity (pmol of phosphate transferred to substrate per 10^5 cells per min at 30°C) in myeloid cells from WT mice at day 4 p.i. with control or DNc parasites. (**E**) Parasitaemia and survival time after inoculation of control or DNc parasites in C57Bl/6 mice issued from a cross between heterozygous RIαB mice and homozygous CD11b/Cre expressor mice; the Cre recombinase activates RIαB expression through removal of an intervening neomycin cassette.

cells (*19*) (Fig. 3A). Key immune modulators affecting trypanosome infection are TNF-α, IFN-γ, and NO (*4*, *5*). In TNF-$\alpha^{-/-}$ mice, the DNc infection pattern reverted to that of control parasites, whereas in IFN-$\gamma^{-/-}$ mice, DNc parasitaemia reverted to control levels after the first peak, and in inducible nitric oxide synthase–negative (iNOS$^{-/-}$) mice, no reversion occurred (Fig. 3, B to D). Infection phenotype reversion in TNF-$\alpha^{-/-}$ mice was specific to DNc parasites because it was not observed with other subvirulent transgenic *T. brucei* lines (fig. S6). Infection phenotype reversion also occurred for induced DNi trypanosomes upon clodronate treatment or growth in TNF-$\alpha^{-/-}$ mice, but not in nude mice (fig. S7). Thus, TNF-α was involved in the effects of trypanosome ACs on infection.

Splenectomy did not affect the DNc infection phenotype (fig. S5), presumably because in mice, the major site of trypanosome interaction with myeloid cells is the liver (*20*). At day 4 post-injection (p.i.), the number of liver TNF-α–synthesizing CD11b$^+$ cells was higher with DNc than with control parasites (Fig. 4A). Specifically, with both parasites, the number of inflammatory monocytes (IMs) (CD11b$^+$/Ly6c$^+$/CD11c$^-$) and inflammatory dendritic cells (IDCs) (CD11b$^+$/Ly6c$^+$/CD11c$^+$) significantly increased while the number of macrophages (CD11b$^+$/Ly6c$^-$/CD11c$^-$) decreased, but in all subpopulations, the percentage of TNF-α–synthesizing cells was ~2.5 times as high with DNc than with control parasites (Fig. 4A). Thus, parasite AC inactivation was linked to early expansion of liver TNF-α^+ myeloid cells.

To evaluate whether the effects of ACs required direct parasite interaction with myeloid cells, monomorphic trypanosomes expressing GFP (WT-GFP) or AC-GFP fusion protein (induced DNi-2) were used. To ensure proper comparison, all mice were treated with doxycyclin. In myeloid cells associated with GFP-labeled trypanosomes at day 3 p.i. (3% of the population) (Fig. 4B), the intracellular level of TNF-α was 2 to 4 times as high with induced DNi than with WT parasites (Fig. 4C and fig. S8). Thus, myeloid cell–associated parasite AC activity was linked to reduction of TNF-α synthesis.

Because cAMP-mediated activation of protein kinase A (PKA) can inhibit TNF-α synthesis (*21*), we measured the PKA activity in CD11b$^-$ and CD11b$^+$ cells from WT mice 4 days p.i. with control or DNc parasites. Increased PKA activity was only observed in CD11b$^+$ cells after control parasite infection (Fig. 4D). Reciprocally, the influence of myeloid cell PKA on infection was addressed. PKA was down-regulated in CD11b$^+$ cells by Cre-mediated activation of a dominant negative regulatory PKA subunit (RIαB) (*22*). Compared with control mice, in RIαB/Cre mice parasitaemia was reduced by a factor of 2.5 (Fig. 4E). Thus, myeloid cell PKA affected trypanosome infection and could be targeted by parasite ACs.

The increased host survival time observed with DNc parasites was associated with reduced liver damage and drastically reduced serum levels of pathogenic TNF-α (fig. S9). This presumably resulted from lower IFN-γ–dependent myeloid cell activation linked to the very low parasitaemia and subsequent low release of VSG (*3*, *4*). In IFN-$\gamma^{-/-}$ mice, the reduction of systemic TNF-α (fig. S9B) could account for increased parasitaemia after the first peak and consecutive reduction of host survival time (compare Figs. 3C and 2B).

Our results indicate that ~50% of total *T. brucei* AC activity is not essential for parasite growth but is crucial to regulate processes involved in parasitaemia control. Specifically, AC activity of trypanosomes, whether triggered upon phagocytosis by the acidic phagosome environment or by trypanolysis, appeared to reduce the early innate defense against live parasites before the massive release of immunomodulatory factors such as VSG GPI anchor fragments at the first parasitaemia peak. Even a few trypanosomes or dead trypanosomes are able to durably affect host innate immunity (*23*). *T. brucei* ACs inhibited TNF-α synthesis in liver myeloid cells, linked to activation of myeloid cell PKA. This evokes the effects of AC toxins from extracellular pathogenic bacteria (*Bordetella pertussis* and *Bacillus anthracis*) (*24*), but contrasts with TNF-α induction by AC from intracellular *Mycobacterium tuberculosis* (*25*).

TNF-α was found to be crucially involved in controlling trypanosome parasitaemia. However, systemic TNF-α did not seem to affect late infection. Thus, the trypanosome-controlling activity of TNF-α would occur early and be restricted to the environment of TNF-α–producing cells. Myeloid cell–proximal TNF-α is thought to facilitate parasite phagocytosis in niches such as the liver, the major organ for trypanosome clearance (*5*, *20*, *23*). Therefore, at the beginning of infection, liver myeloid cells could target most invading parasites, and without efficient parasite AC response, only low parasitaemia could develop in the blood.

The AC function at the host-parasite interface would explain the specific expansion and diversification of ACs in extracellular trypanosomes continuously exposed to the immune system. This conclusion could also apply to other extracellular parasites such as *Trichomonas vaginalis* (*26*). The sequence diversity of the AC extracellular domain might help to prevent efficient recognition by antibodies. Examples of polymorphism associated with parasite enzymes exposed to the immune system include the *T. cruzi* transsialidases (*27*) or the *Toxoplasma gondii* protein kinases (*28*).

References and Notes

1. E. Pays, L. Vanhamme, D. Pérez-Morga, *Curr. Opin. Microbiol.* **7**, 369 (2004).
2. S. Rolin *et al.*, *J. Biol. Chem.* **271**, 10844 (1996).
3. S. Magez *et al.*, *J. Immunol.* **160**, 1949 (1998).
4. J. M. Mansfield, D. M. Paulnock, *Parasite Immunol.* **27**, 361 (2005).
5. S. Magez, M. Radwanska, A. Beschin, K. Sekikawa, P. De Baetselier, *Infect. Immun.* **67**, 3128 (1999).
6. M. Guilliams *et al.*, *J. Immunol.* **182**, 1107 (2009).
7. S. Magez, B. Stijlemans, T. Baral, P. De Baetselier, *Microbes Infect.* **4**, 999 (2002).
8. S. Alexandre *et al.*, *Mol. Biochem. Parasitol.* **77**, 173 (1996).
9. D. J. Bridges *et al.*, *Proteomics* **8**, 83 (2008).
10. D. Salmon *et al.*, *Mol. Microbiol.* **84**, 225 (2012).
11. E. Pays *et al.*, *Cell* **57**, 835 (1989).
12. S. Alexandre *et al.*, *Mol. Biochem. Parasitol.* **43**, 279 (1990).
13. C. Naula, R. Schaub, V. Leech, S. Melville, T. Seebeck, *Mol. Biochem. Parasitol.* **112**, 19 (2001).
14. T. Seebeck, R. Schaub, A. Johner, *Curr. Mol. Med.* **4**, 585 (2004).
15. H. P. Voorheis, B. R. Martin, *Eur. J. Biochem.* **113**, 223 (1980).
16. B. Bieger, L. O. Essen, *EMBO J.* **20**, 433 (2001).
17. P. Paindavoine *et al.*, *Mol. Cell. Biol.* **12**, 1218 (1992).
18. L. Lecordier *et al.*, *Mol. Biochem. Parasitol.* **140**, 127 (2005).
19. N. Van Rooijen, A. Sanders, *J. Immunol. Methods* **174**, 83 (1994).
20. W. L. Dempsey, J. M. Mansfield, *J. Immunol.* **130**, 405 (1983).
21. E. A. Wall *et al.*, *Sci. Signal.* **2**, ra28 (2009).
22. B. S. Willis, C. M. Niswender, T. Su, P. S. Amieux, G. S. McKnight, *PLoS ONE* **6**, e18772 (2011).
23. G. Wei, H. Bull, X. Zhou, H. Tabel, *J. Infect. Dis.* **203**, 418 (2011).
24. K. A. McDonough, A. Rodriguez, *Nat. Rev. Microbiol.* **10**, 27 (2012).
25. N. Agarwal, G. Lamichhane, R. Gupta, S. Nolan, W. R. Bishai, *Nature* **460**, 98 (2009).
26. J. Cui, S. Das, T. F. Smith, J. Samuelson, *PLoS Negl. Trop. Dis.* **4**, e782 (2010).
27. L. Ratier *et al.*, *PLoS ONE* **3**, e3524 (2008).
28. J. P. J. Saeij *et al.*, *Science* **314**, 1780 (2006).

Acknowledgments: We thank S. McKnight and P. Amieux (University of Washington) for the RIαB mice and helpful suggestions; O. Leo (IBMM, Gosselies) for excellent advice; and D. Monteyne, P. Poelvoorde, M. A. Laute, E. Omasta, and P. Tebabi for technical assistance. This work was supported by the Belgian Fund for Scientific Research (FRSM), the Wallonie-Bruxelles International/Fundação Coordenação de Aperfeiçoamento de Pessoal de Nível Superior (CAPES) bilateral cooperation agreement, the Jean Brachet Fund, the Interuniversity Attraction Poles Programme–Belgian Science Policy, German Research Foundation (DFG) grant 1100/7-1, and the University of Munich. The trypanosome DNA sequences can be retrieved from release 4.0 of the TriTrypDB (www.tritrypdb.org) and NCBI GenBank. The kinetoplastid AC sequence alignments and accession nos. have been deposited at TreeBase (http://purl.org/phylo/treebase/phylows/study/TB2:S12552). Author contributions: D.S., G.V., M.B., A.B., and E.P. conceived the work; D.S., G.V., Y.M., J.D., C.K., F.L., S.B., J.G., M.K., F.B.S.D., G.D.M., P.U., S.M., and J.V.D.A. performed experiments; D.S., M.M., P.D.B., M.B., A.B., and E.P. supervised different aspects of the experimental plan; and E.P. wrote the paper. The authors declare that they have no competing financial interests.

Supplementary Materials

www.sciencemag.org/cgi/content/full/science.1222753/DC1
Materials and Methods
Figs. S1 to S9
Table S1
References (*29*–*41*)

2 April 2012; accepted 1 June 2012
Published online 14 June 2012;
10.1126/science.1222753